XXIV LATIN AMERICAN CONGRESS ON HYDRAULICS
PUNTA DEL ESTE, URUGUAY, NOVEMBER 2010

VORTEX DETECTION IN PUMP SUMPS
BY MEANS OF CFD

Cecilia Lucino, Sergio Liscia y Gonzalo Duró
Laboratorio de Hidromecánica – Área Departamental Hidráulica – Facultad de Ingeniería
Universidad Nacional de La Plata, Argentina
clucino@ing.unlp,edu.ar; soliscia@ing.unlp,edu.ar; gzduro@gmail.com

RESUMEN:

El trabajo tiene como finalidad verificar la capacidad de un modelo matemático comercial de fluidodinámica computacional (CFD) para predecir la formación de vórtices en una dársena de bombeo. Se propone identificar vórtices de distinto origen e intensidad en una dársena de bombeo de geometría sencilla, de la cual se cuenta con resultados experimentales de las mismas condiciones de operación. Las velocidades calculadas muestran tendencias y magnitudes similares a las medidas, mientras que los valores máximos de vorticidad calculados resultan varios órdenes mayores que los medidos, lo cual se explica por las características de la medición en modelo físico.

La modelación predice la presencia de vórtices superficiales cuya ocurrencia fue detectada en el modelo físico de referencia, pero además detecta vórtices de pared y de fondo que no fueron registrados en el trabajo de referencia. La representación de la vorticidad total, expresada por su valor absoluto, y seleccionada como superficie equipotencial, resulta ser una herramienta de visualización muy útil para realizar un seguimiento de la ubicación, trayectoria y variación temporal de los vórtices concentrados.

ABSTRACT:

The present work is aimed at verifying the ability of a commercial computational fluid dynamic (CFD) code to predict the formation of vortices in a pump sump. It was intended to identify vortices of diverse origin and intensity in a geometrically simple pump sump of which experimental results under the same operating conditions are known. Calculated velocities correlate well to trends and magnitudes of measured ones, whereas the maximum values of vorticity calculated are several orders of magnitude higher than those measured, which is explained by the characteristics of measurement in the physical model.

Model results predict the presence of surface vortices which were seen in the reference physical model, but also wall vortices and floor vortices which were not reported in the reference work under the same working conditions. For lower submergences, the presence of the floor vortex in the physical model is inferred from the cavitation in the core. The representation of total vorticity, in terms of its absolute value, and selected as an equipotential surface, may turn into a very useful tool to visualize and follow the actual location, trajectory and time variation of concentrated vortices.

KEY WORDS:

Vortex, pump sump, air entrainment

INTRODUCTION

The experience in testing over physical models in the pumping installations of the Hydraulic Department (Faculty of Engineering of the National University of La Plata) shows that in most cases the verification of a design in these models demands quite time and resources. There is no doubt that it is convenient to make a progress in the diagnostic of design problems before taking it to the verification stage in the physical model.

Over time, the hydromechanics facilities have reached such dimensions, as well as the magnitudes of the pumped flow rate, that the deficits in the design generate worse hydrodynamic consequences. These bigger scales of hydraulic constructions positions CFD modeling as a useful tool in different project stages of a pump station, especially since the availability of *workstations* (independent computational systems of great processing capacity and high graphic capacity) that have reduced the processing time of the solvers.

The appearance of vortices in pump sumps and their negative consequences to the facilities is maybe the most common problem found in these type of installations and at the same time the most complex to solve, especially when there are multiple pumps and the flux entrance is strongly restricted due to context conditions (such as closed curves, reduced sections, etc.).

To make a progress in this way, the work proposes the validation of the mathematical model of commercial use called FLOW-3D$^{®}$ at a geometrically simple pump sump. Additionally, conclusions and propositions of necessary studies are set to take advantage of the possibilities that this software offers.

OBJECTIVES

The work is aimed at the validation of the mathematical model of commercial use FLOW-3D$^{®}$ for the representation and identification of vortices of different origin and intensity in a pump sump of simple geometry, of which there are experimental measurements in the same operating conditions.

METHODOLY

CFD model

FLOW-3D$^{®}$ was developed by Flow Science Inc. in the United States and it is a code that simulates fluid dynamics based on the numerical solution of the Navier-Stokes ecuations and continuity. It also has several auxiliary models to solve different kinds of situations like sediment transport, moving rigid bodies, flows in porous media, etc. The free surface is tracked by means of the VOF method (Volumen Of Fluid) and the model uses the FAVOR$^{®}$ method to determine the solid boundaries.

For the simulation of the sump three linked meshes were used and all of them had cubic cells. In the first place, a mesh was located at beginning of the channel with eight millimeters high cells. Then, a mesh with four millimeters high cells was positioned in the pump area where a more detailed analysis of the flow was of interest. At last, a mesh of four millimeters high cells was situated at the upper part of the pump in order to impose the boundary condition of the desired volume flow rate. To make one thing clear, it was only used four millimeters cells in the pump environment with the aim of reducing the amount of total cells, because its number has a direct influence in the duration of the solver calculations.
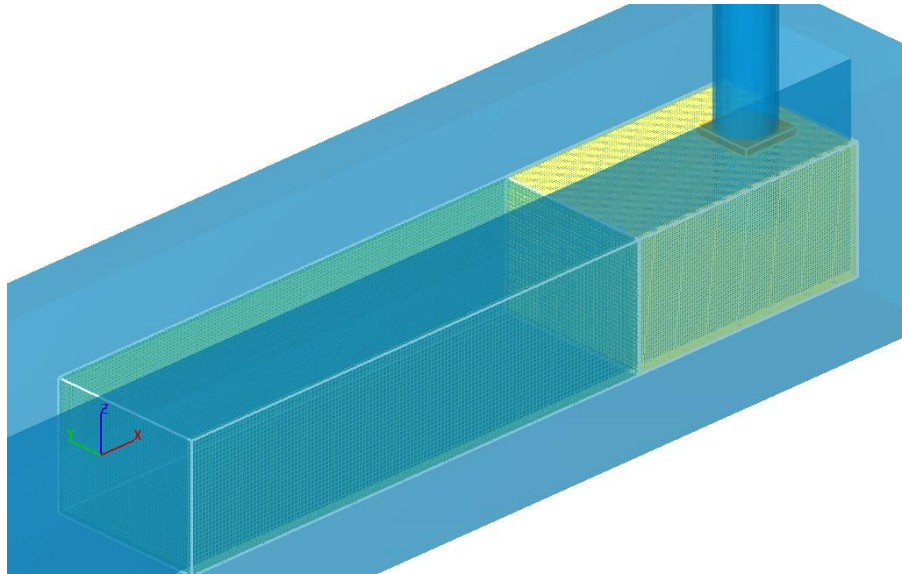
Figure 1. - Meshes used in the modeling

To sum up, the number of cells of the first mesh, the green one in **Figure 1**, was 167680; the second mesh (yellow) had 655360 cells and the third mesh (orange) had 3600 cells.

The modeled length of the channel was established considering the minimum necessary distance for the complete development of the boundary layer before the flow reached the pump, since the flow at the inlet has a uniform velocity distribution.

The boundary condition at the inlet consisted of a total hydraulic head equal to the aimed water elevation plus three millimeters. The latter was due to the head loss until the flow reached the pump.

The boundary condition at the outlet was a constant volume flow rate going out of the domain. This was located at the top face of the orange mesh in **Figure 1**.

The fluid was considered monophasic and incompressible, at a temperature of 20ºC. The physical models activated were gravity and turbulence. The gravity acceleration was set to 9.81 m/s² and the turbulence model used was the Large Eddy Simulation. A third order of approximation was utilized to calculate the momentum advection, and the Split Lagrangian was the method chosen for the advection of the VOF.

Vortex observation

The main aspect of this research was to explore the possibilities of the CFD simulation to identify the different kinds of vortex structures that may appear in a pump sump.

The free surface flow confined to a typical pump sump geometry presents certain particularities. On the one hand, there is an interphase water-air, restricted by the shape of the solid boundaries of the walls that force changes in the direction and the pump itself, that represents an obstacle for the portion of the superficial flux that is not conducted in a direct way to the pump bell and goes to the space located behind the pump. Under specific conditions, the flow organizes into surface vortex, coherent structures, with different levels of stability that depend on the submergence and the characteristics of the approach flow.

On the other hand, the submerged flow is subject to the changes of direction and magnitude of the velocity imposed by the pumping and the geometry of the solid boundaries. In this process, in which local fluxes with circulation components are induced, the boundary layer near the solid surfaces gives the flux additional circulation, resulting in floor and wall vortices that may be very stable. Unlike surface vortices, the presence of these submerged vortices does not directly depend on the submergence. However, the increase of the flow velocity, which can occur with a lower

submergence at equal flow rate, may result in cavitating states of the submerged vortices (Iwano, 2002). This was observed in the test under different operating conditions. The level of local depression in the vortex core when limit velocities are reached implies cavitation, which enters in the suction bell and leads to negative consequences for the pump.

In complex geometries designs, there are combined effects that come from the lack of uniformity in the velocity profile of the approach flow, factors of the geometry itself, submergence and flow guiding in the environment of the pump. In these cases, it is difficult to analyze the multiple factors which overlap and result in an inefficient functioning of the set and therefore it is laborious and costly to seek for corrective actions. For this reason, it is proposed to explore techniques for visualization of vortex structures in a simple geometry, from which experimental data is known to validate their results.

Benchmark test

It was taken as a reference the physical model test presented by Matsui (2006) and Okamura (2007) which consists of a simple geometry, with the pump situated with an eccentricity of 3% of the sump width from the center of the sump passage (**Figure 2**). The work documents the comparison between experimental results with numerical ones from different CFD codes. The measurements were performed using the PIV (Particle Image Velocimeter) technique and also a laser light sheet method was used to locate the vortices. Images of the velocity field, vorticity field, as well as residence time and location of vortices were presented.

From the publication only the measured data in the physical model was taken into account for its analysis, not considering the CFD results because it exceeded the scope of this work.

The results of a first stage are presented which correspond to a pumped flow rate of 1 m³/min and a water level of 230 millimeters. Also a second stage test consisting of a water level of 150 millimeters and the same flow rate is shown with the aim of anticipating the trends of the simulation and its coincidence with the measured values.
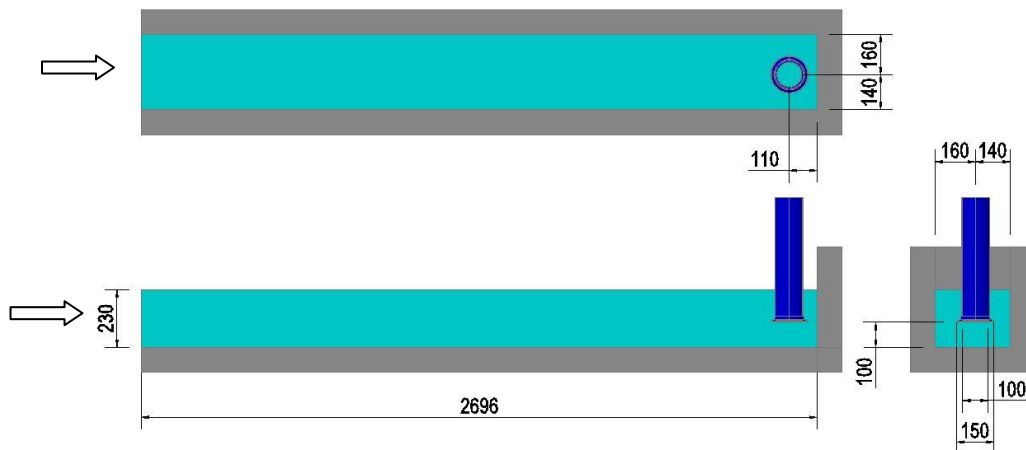
Figure 2.- Geometry of the reference physical model (Matsui, 2007)

The boundary conditions used in the simulation of the first stage were a constant water level of 230mm at the inlet section and a constant flow rate of 1 m³/min at the upper section of the pump.

The computing time is a concrete limitation so it is necessary to find an adequate mesh size that may represent the expected phenomena to be analyzed in a reasonable processing time. To this end, we conducted the following procedure:

a) Two simulations were performed consecutively: the first one with a structured mesh of cubic cells that were 8 millimeters high to arrive at a steady state condition. From this simulation it was taken a velocity profile as the boundary condition at the inlet for the next simulation that had 4 millimeters high cells. This was 60 seconds long, and from it the post-processing was performed arriving at the results that later on are shown.

b) Another simulation was performed with cubic cells of 8 millimeters high during 400 seconds to perceive the temporal variation of the vorticity in the pump surroundings. The post-processing of these results which consisted of animations allowed to compare the location of the vortices with the ones observed in the physical model.

RESULTS

Comparison of velocities and vorticity

In **Figures 3**, **4** and **5** calculated velocities are presented in a reference section where measurements were performed in the physical model. The presented results correspond to a mesh of 4 millimeters high cells (instantaneous values), a mesh of 4 millimeters high cells (averaged values of a 60 seconds period), a mesh of 2 millimeters high cells (averaged values of a 5 seconds period) and the measured values in the physical model. These results correspond to the bell inlet section at 85 millimeters from the sump floor that cuts the center of the pump, shown in **Figure 6**. The latter also shows a CFD result from a top view of the sump that consists of the velocity magnitude and the vectors in the plane.

The tendencies of the calculated and measured velocities are coincident. Also, in general theirs magnitudes are similar. It can be observed that the simulation with the 4mm cells reproduces the same tendency as the 2mm cells but the former shows larger magnitudes than the latter (it must be remembered that with the 2mm cells it was only reproduced the mean value of a 5 seconds period).

For the studied section, the calculated velocity u (the x direction is positive in the sense of the mean flow) presents a difference with the measured one that has influence in the representation of the floor vortices. In the CFD results, the change in the sense of the velocity, ranging from positive to negative values, is compatible with the formation of two floor vortices that enter the pump swirling in opposite directions. The existence of this phenomenon does not appear in the reference article.

Figure 7 presents the vorticity ω at the same location. It can be noticed that the calculated values are significantly higher than the measured ones, especially for the mesh with 4mm cells. An explanation for this is that the technic employed for the measurement (PIV) considers averaged values of the velocity instead of instant values (Nagahara, 2003). In **Figure 8** the velocity components u and v, and the vorticity ω were overlaid with the aim of clearly appreciating the vortex core of higher magnitude. Despite the presence of two vortices that interact with each other and distort their velocity profile, it can be seen that the one with negative values of vorticity ω, at its core there is a forced vortex behavior, and since a radius of approximately 1.5 cm (the peak of u and v velocities) there is a free vortex behavior.
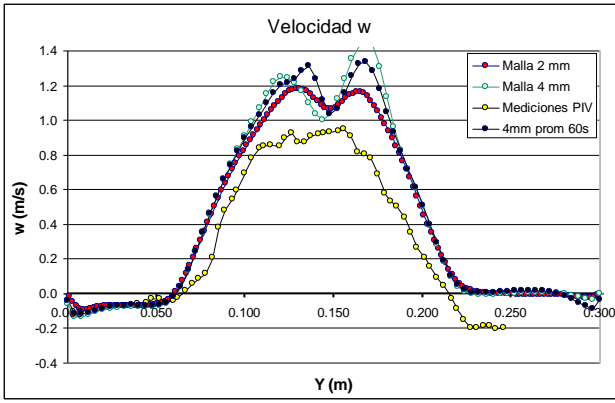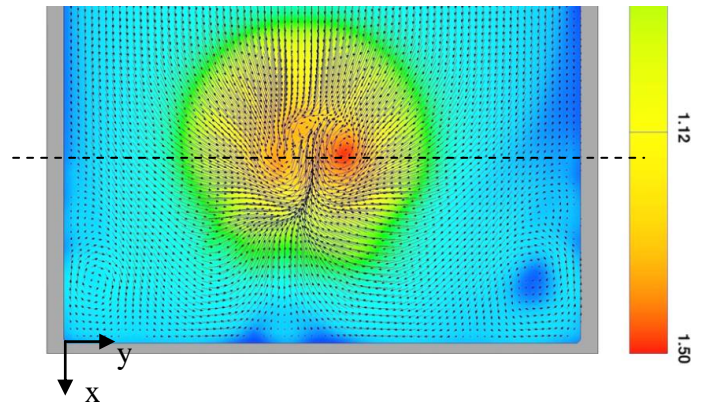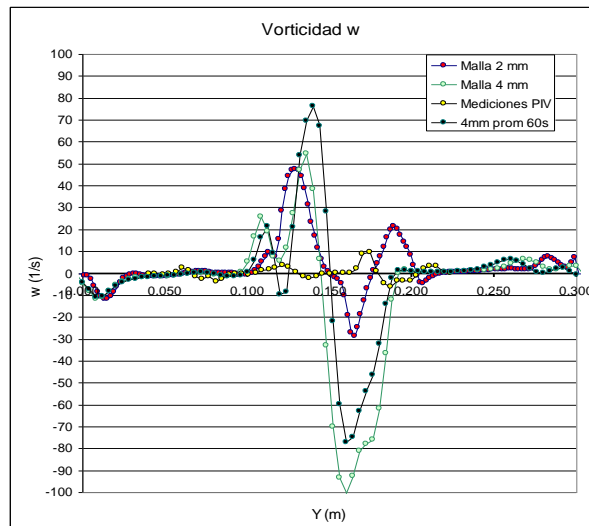
Figure 3.- Velocity w (section Z=0.85 m)
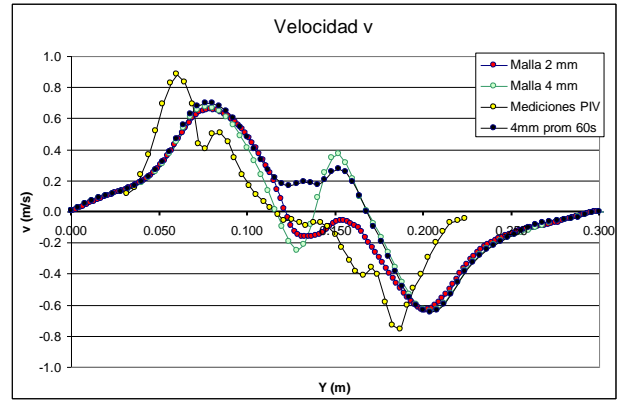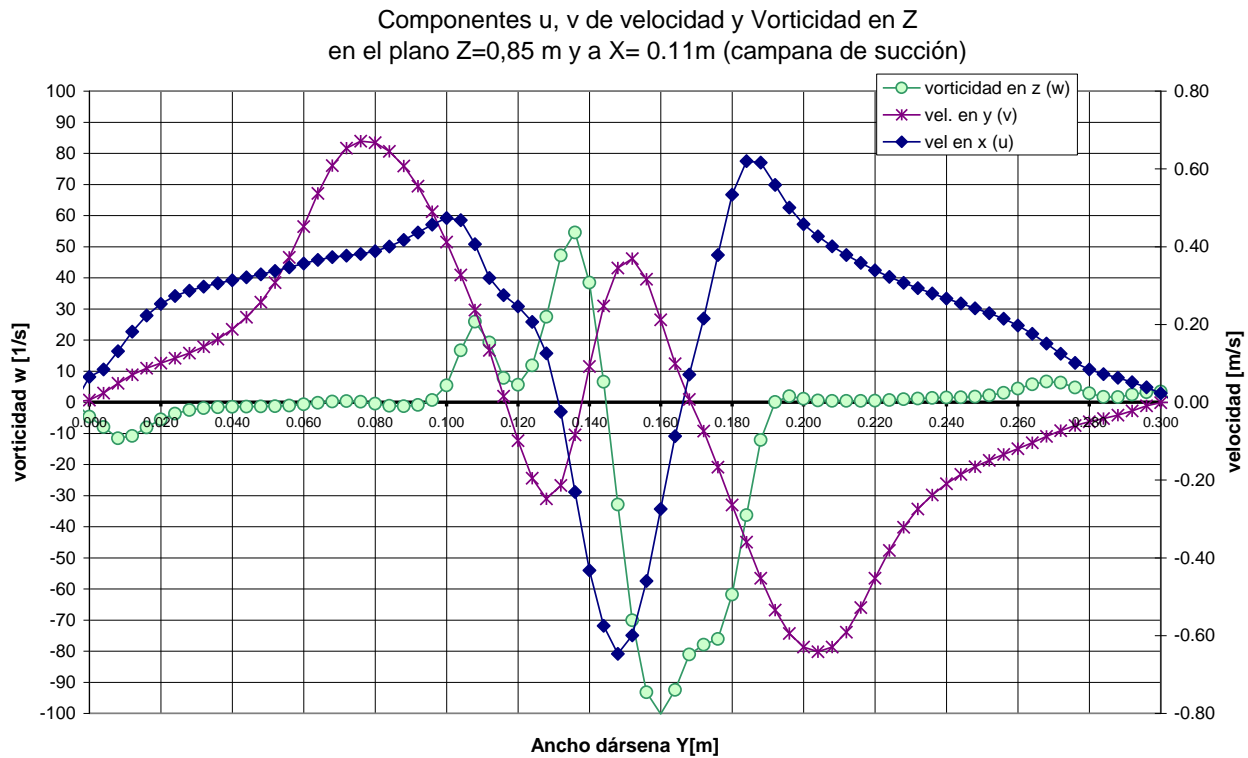

Figure 4.- Velocity v (section Z=0.85 m)
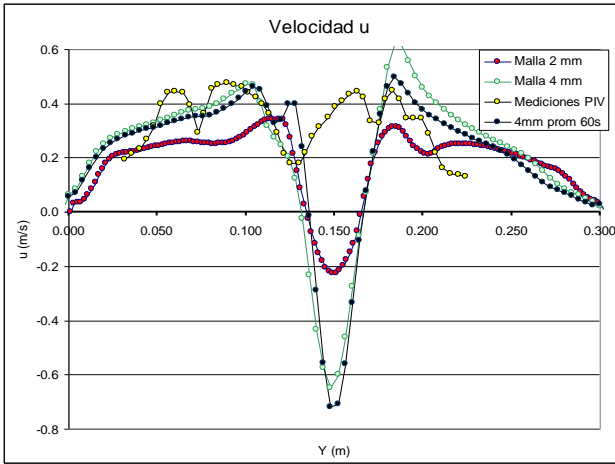
Figure 5.- Velocity u (section Z=0.85 m)

Figure 6.- Velocity magnitude in section Z=0.85 m

Figure 7.- Vorticity ω (section Z=0.85 m)

Figure 8.- Velocities u and v associated to the vorticity ω in section Z=0.85 m

Qualitative comparison of different types of vortices

The post-processing of the results was made using streamlines, the vorticity field, the velocity field and the deformation of the free surface.

To evaluate the tendency to the formation of vortices with potential air entrainment in the pump environment, the indicators considered were the vorticity magnitude, the permanence in time of that vorticity as a coherent structure, and the velocity gradient in the helical path to the pump.

Vortices that are hard to detect in a direct way in the physical model may be appreciated with the CFD with adequate methods of visualization to capture their structure. The vortices that are intended to be identified are coherent structures which vorticity magnitude is above the vorticities of the rest of the fluid. Since this concept it was led to represent surfaces with a constant value of vorticity (the magnitude or a specific direction of interest), step by step increasing it until the vortices are isolated, thus being able to identify its structure and permanence.

In the physical model for the studied case, it was recorded the presence of an air-entrained vortex with a permanence of the 70% of the time (**Figures 9** and **10**). It was located between the pump and the back wall, at the right side with a downstream view.

With the CFD, by means of the described method of visualization, it was found that the greatest organized vorticity in the z direction with a connection to the free surface was located at the same place that was observed in the test (**Figure 11**). The variation of the colours at its structure represents the velocity w (in the z direction). This gradient of the velocity to the pump bell makes probable that at a certain level might produce air entrainment. Another vortex is also present at the left corner but with lower intensity from which there is no reference in the benchmark work that can be seen in F**igures 11** and **12**. In **Figure 13** streamlines that enter into the surface vortex are shown. For this purpose the streamlines were planted until they reached the zones of interest.

The magnitude of the vorticity and the depression of the free surface in a permanent and stable way indicate the potential air entrainment, even though the code does not represent its real magnitude. This aspect will be investigated in the next phase of studies.
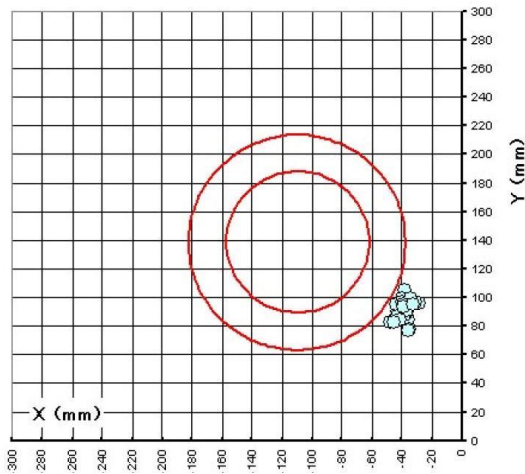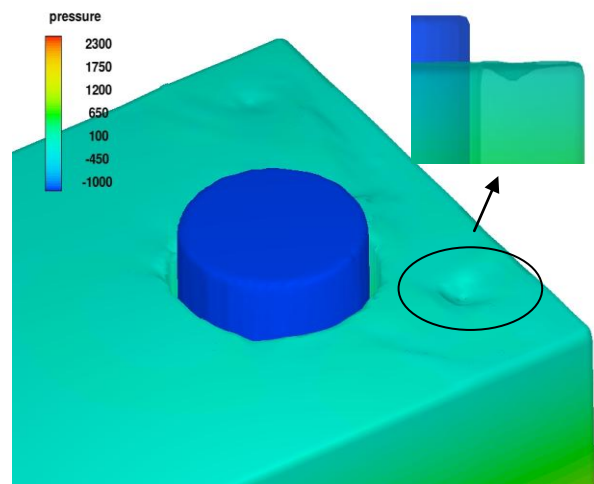
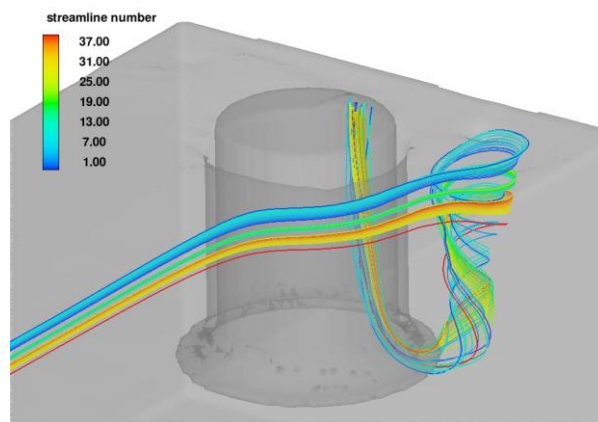**Figure 9.-** Location of the air-entrained vortex (Matsui, 2007)
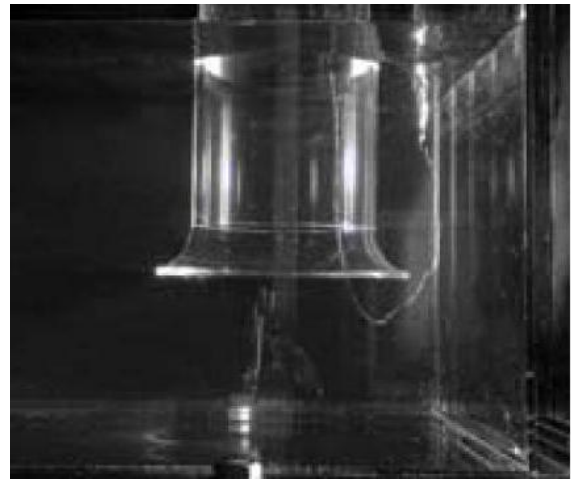
Figure 10.- Air-entrained vortex in the physical model – Side view (Matsui, 2007)
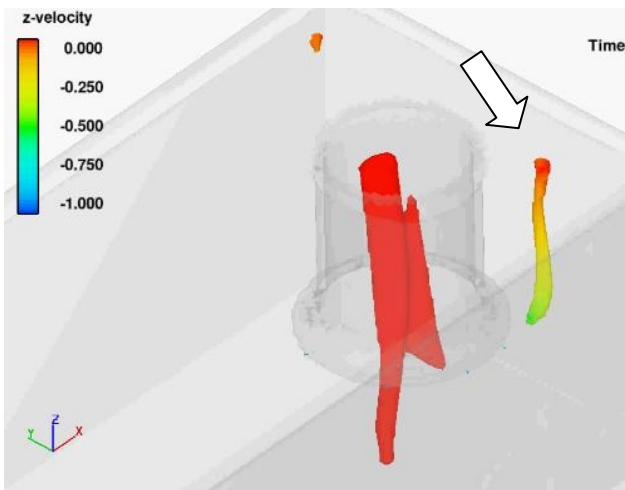
Figura 11.- Surfaces of equal vorticity ω (60 1/s) coloured by velocity z


Figura 12.- Surface depression

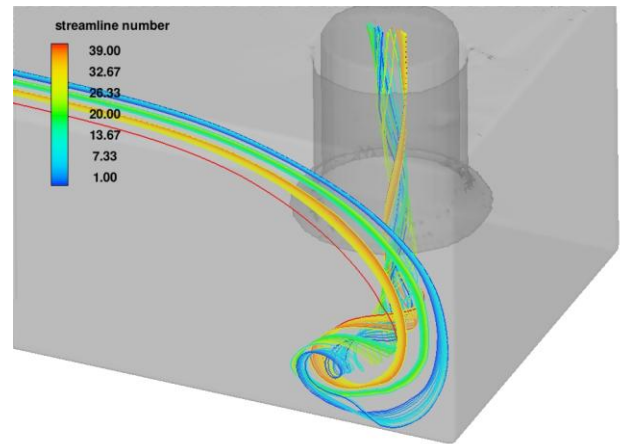**Figura 13.-** Streamlines in the surface vortex

The CFD code also predicted the presence of submerged vortices, wall and floor ones, which were not described in the reference publication for the studied case.

It is worth mentioning that in the experiments that followed the one presented here, lower submergence conditions were established that induced the appearance of a cavitating submerged vortex, so it can be inferred that this vortex already existed in the previous condition of higher submergence, but it had not been detected.

In **Figure 14** it can be seen the two mentioned vortices, one located at the wall and the other under the pump bell. The wall vortex was also detected with streamlines and it is shown in **Figure 15**.
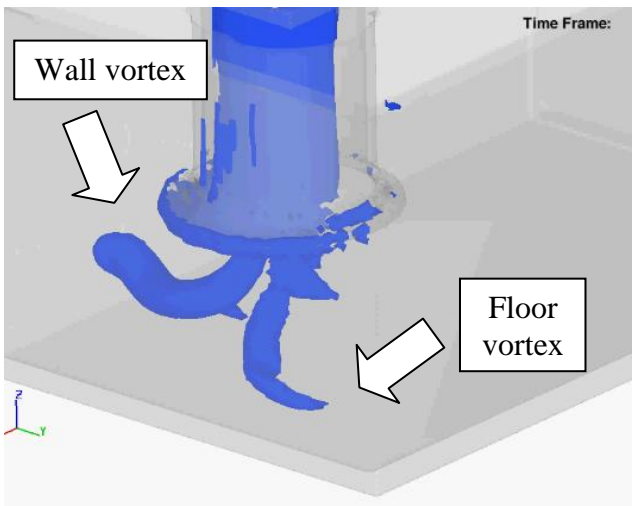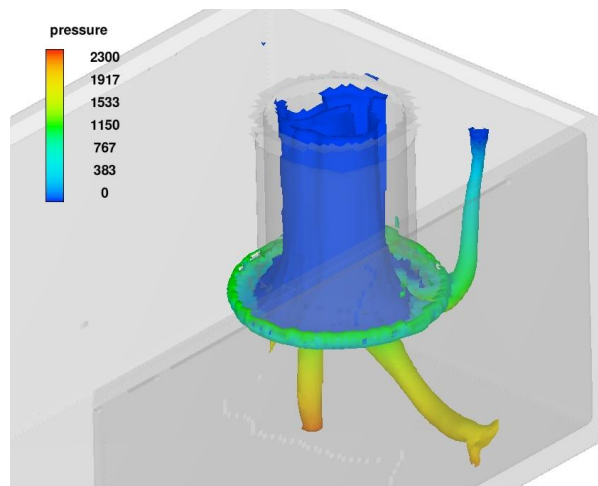

Figure 14.- Wall and floor vortices

Figure 15.- Streamlines at the wall vortex

Figure 16 shows an instant when the three mentioned vortices coexist at the same time.


Figure 16.- Floor, wall, and surface vortices

Results with a lower submergence

Results of a different operating condition are presented below. The flow rate stays the same, 1 m³/min, but the water depth is 150mm. The calculated results are compared with the observations made at the physical model. A photograph of this situation is shown in **Figure 17** which was published in the reference article. It can be appreciated that a cavitating submerged vortex is coexisting with an air-entrained one.

At the left side of **Figure 18** there is an image of the simulation where the superficial vortices have the same location as the recorded in the physical model. It can be observed that the proposed code cannot depress the free surface enough to make "air" enter the pump.

For this operating condition the code shows that the vortices are unstable and their locations are variable in time as was measured in the test. Also it can be noticed that the free surface depression corresponding to the corner vortex disappears, probably due to the disturbances of the flow in this area as a consequence of the higher velocities. The locations of the detected vortices in the physical model are presented in **Figure 18** (right).

The floor vortex in the CFD has an unstable position. **Figure 19** shows an instant image of the pressure field at section Z=0.85m where there are the pressures below the atmospheric pressure, even they do not reach the vapor pressure.
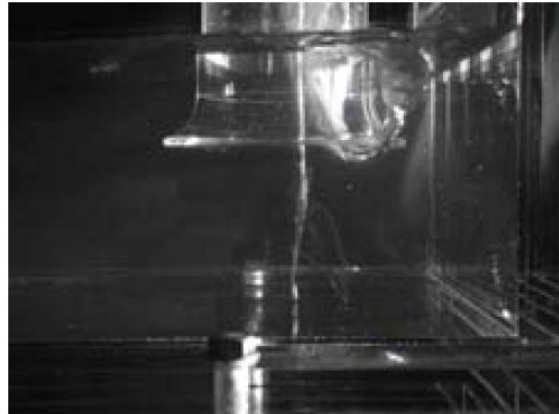
Figure 17.- Submerged vortex and air-entrained vortex with lower submergence(Matsui, 2007)
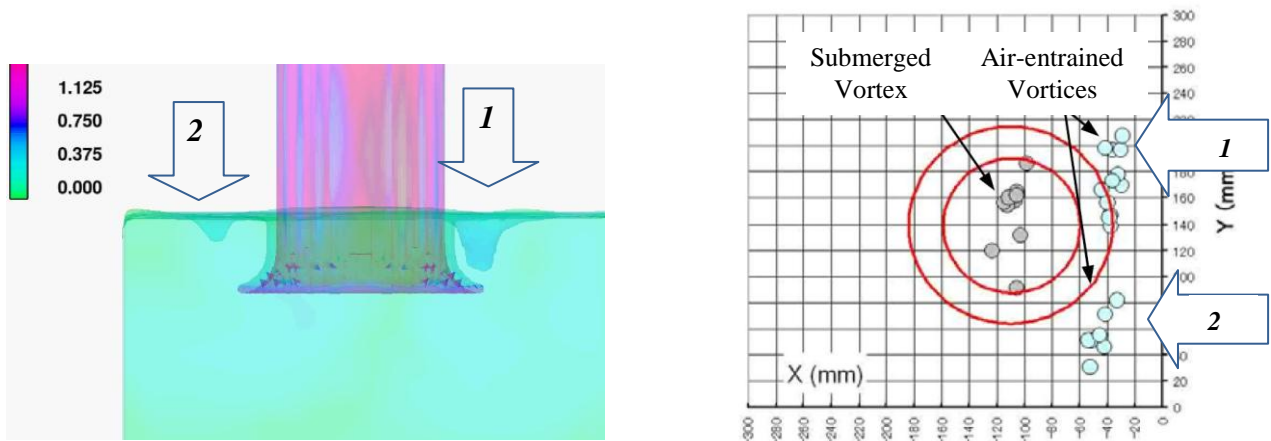
Figure 18.- Free surface depressions in the CFD, back view (left). Measured locations of air-entrained vórtex core and submerged vortex core, top view (Matsui, 2007) (right)
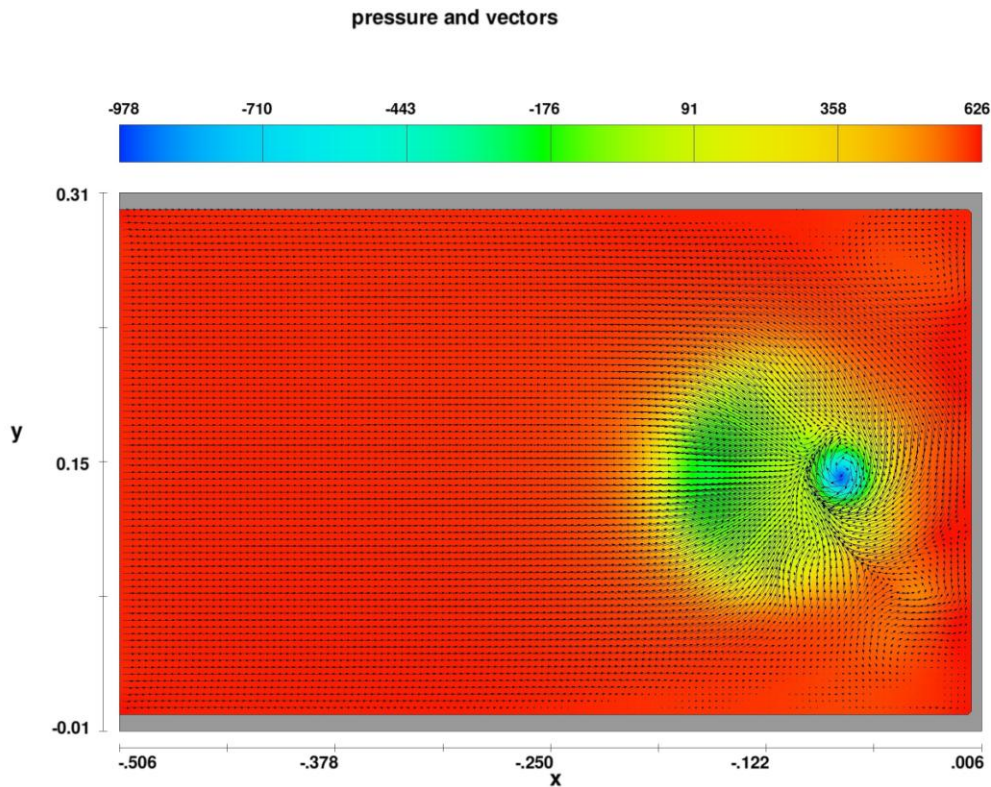
Figure 19.- Depression in the floor vortex

CONCLUSIONS

The presented results allow establishing some conclusions regarding the application of the FLOW-3D® code for detecting vortices in a pump sump using the LES (Large Eddy Simulation) model. The latter has been suggested in the references (Tokyay, 2005) instead of other turbulence models like the Reynolds Averaged Navier-Stokes (RANS) which does not represent in a realistic way the highly unstable and intermittent phenomenon. The numerical results demonstrate the capability of the model identifying the observed vortices in the physical model. It is verified that the calculated vorticities with the highest values are consistent with the air-entrained vortices. The floor vortex reaches the highest vorticity magnitude and suggests the possibility of a cavitating core at the operating condition of lower submergence. This was confirmed in the physical model. On the other hand, it was found that the iso-surfaces of high values of vorticity are a useful tool for the appreciation of the structures of surface, floor and wall vortices.

The use of a monophasic fluid instead of a biphasic one has the advantage of consuming less time. Therefore some authors propose the application of post-processing techniques based on theoretical models of vortices (Iwano, 2002; Chen, 2007) to predict the conditions of air entrainment or the existence of cavitation in vortex cores. The convenience of these alternative post-processing techniques will be analyzed in the next stage of studies.

REFERENCES

Chen Y., Wu Ch., Ye M., Ju X. (2007) Hydraulic Characteristics of Vertical Vortex at Hydraulics Intakes Journal of Hydrodinamics, Ser.B, 2007,19(2):143-149.

Iwano, R., Shibata T. (2002). "Numerical prediction method of submerged vortex and its application to the flow in pump sumps and without a baffle plate". *Proceedings of the 9th*

International Symposium on Transport Phenomena and Dynamics of Rotating Machinery. Honolulu, Hawai,

Matsui J., K. , Okamura T. (2006). "CFD Benchmark and a Model Experiment on the Flow in a Pump Sump". *Proceedings of 23rd IAHR XXIX Symposium*, Yokohama, Japan.

Nagahara, T., **Sato T., Okamura T.** (2003), "Measurement of the Flow around the Submerged Vortex Cavitation in a Pump Intake by Means of PIV", Fifth International Symposium on Cavitation. Osaka. Japan. P 1-7

Okamura T., Kyoji K. and Matsui J. (2007). "CFD Prediction and Model Experiment on Suction Vortices in Pump Sump". *Proceedings of the 9th Asian International Conference on Fluid Machinery*. Jeju, Korea.

Tokyay, T. and Constantinescu, S.G. (2005), "Large Eddy Simulation model to simulate flow in pump intakes of realistic geometry. II: Investigation of dynamics of coherent structures", Journal of Hydraulic Engineering, ASCE.